CHAPTER III

PREPARATION OF HYDROLYZED ELECTROSPUN POLYACRYLONITRILE FIBER MATS AS CHELATING SUBSTRATES: A CASE STUDY ON COPPER(II) IONS

3.1 Abstract

Ultrafine polyacrylonitrile (PAN) fiber mats were prepared by electrospinning and they were hydrolytically-treated with a sodium hydroxide solution to impart the ability to chelate metal ions. This was achieved through the conversion of the nitrile functional groups on the surface of the PAN fibers into imine conjugated sequences, which was confirmed by Fourier-transform infrared spectroscopy. The chelating property of the hydrolyzed electrospun PAN fiber mats (i.e., H-ePAN fiber mats) was evaluated against Cu(II) ions. The amounts of the Cu(II) ions adsorbed onto the H-ePAN fiber mats were influenced by the initial pH and the initial concentration of the metal ion solutions. At the optimal pH of 5.0, the amounts of the Cu(II) ions adsorbed onto the H-ePAN fiber mats increased with an initial increase in the time the materials were in contact with the metal ion solution to finally reach the maximal, plateau values after about 5 h of immersion. The maximal adsorption capacity of the H-ePAN fiber mats for the Cu(II) ions was determined to be 31.3 $mg \cdot g^{-1}$ and the fully-adsorbed materials could be regenerated upon submersion in 0.1 M hydrochloric acid solution for 30 min. Finally, X-ray photoelectron spectroscopy indicated specific interactions between the adsorbed Cu(II) ions and the N- and/or the O-atoms associated with the imine groups on the surface of the H-ePAN fibers.

(**Key-words**: electrospinning; hydrolyzed polyacrylonitrile; chelating fibers; copper removal)

3.2 Introduction

The presence of heavy metals, such as chromium (Cr), copper (Cu), lead (Pb), mercury (Hg), nickel (Ni), and zinc (Zn), in industrial effluents is of serious environmental concern, which, upon being left untreated, can cause serious illnesses to all living organisms, including humans [1, 2]. Among these, copper (Cu), as a trace element, is essential for the growth of all higher plants, animals and humans. Nonetheless, excessive intake of Cu in humans' results in its accumulation in the liver and prolonged exposure to it could cause gastrointestinal problems, severe headache, hair loss, hypoglycemia, increased heart rates, nausea, and damages to the kidney and the liver [3, 4]. According to the Pollution Control Department of the Ministry of Natural Resources and Environment of Thailand, the maximal acceptable concentration of Cu(II) ions in an industrial effluent must not exceed 2.0 $mg{\cdot}L^{-1}$. The world health organization (WHO) also recommended a maximum acceptable concentration of Cu(II) in drinking water of 1.5 $mg{\cdot}L^{-1}$[5, 6]. Therefore, the removal of the excessive amounts of this metal species from industrial wastewater is mandatory and crucial to humans' welfare.

Various techniques, such as precipitation, electroplating, ion exchange, membrane separation, and adsorption [1, 3, 7–10], have been used as means to remove heavy metal ions from aqueous effluents. Among these, adsorption is one of the most preferred methods, because of its high efficiency and cost effectiveness. There have been many studies on the removal of Cu(II) ions from aqueous solutions using different adsorbents. These adsorbents can be derived from materials of diverse origins, whether naturally or synthetically. Some of these are, for examples, chitosan [11], neat and modified activated carbon [1, 12, 13], and chelating resins [14,15]. The latter can be tailored to exhibit specific selectivity towards certain heavy metal ions, which are made possible through the proper choices of specific chelating groups (e.g., amidoxime, amino, carboxyl, imidazoline, phosphoric, and thioamido groups) [16–23].

Among the numerous adsorbents for metal ions, chelating fibers, due mainly to their ease of handling and high adaptability, is a class of such materials that has

been extensively explored. Various research reports have focused on improving the adsorption capacities and increasing the adsorption rates of certain metal ions on chelating fibers and, at the same time, achieving easy desorption which dictates their reusability. In particular, the preparation of these chelating fibrous materials is relatively simple. Among various fibrous materials, those made of polyacrylonitrile (PAN) can be easily modified to obtain chelating fibers. This is a direct result of the presence of the nitrile groups (C≡N) which are readily modifiable into various chelating groups [24-26]. In 2003, Deng et al. [27] prepared hydrolyzed PAN microfibers that exhibit high adsorption capacity towards Cu(II) ions. It is, therefore, of our interest to develop hydrolyzed PAN fibers, based on the fibers *a priori* fabricated from a process commonly known as electrospinning [28], which is capable of producing ultrafine fibers with diameters ranging from micro- down to nano-meters.

Various types of materials, including polymers, can be facilely made into ultrafine fibers by electrospinning [28]. In the traditional set-up, a polymer liquid (i.e., melt or solution) is loaded into a container with a small opening, i.e., a nozzle, and subsequently charged with a high electrical potential across a finite distance between the nozzle and a grounded collection device. When the electric field exceeds a critical value, a charged stream of the liquid, i.e., a charged jet, is ejected [28]. As the jet travels to the collector, it either cools down or the solvent evaporates to obtain ultrafine fibers in the form of a non-woven fabric on the collector. Various parameters, such as solution properties (e.g., concentration, viscosity, conductivity, surface tension, etc.), processing conditions (e.g., electrical potential, collection distance, etc.), and ambient conditions (e.g., temperature, humidity, etc.), dictate the morphology of the resulting fibers [28–30]. Some proposed uses of electrospun fibers are, for examples, scaffolding materials for cell/tissue culture [31], carriers for DNA and drug delivery [32, 33], and active membranes [34].

In the present contribution, electrospinning was used to prepare non-woven matrices of ultrafine fibers from commercial PAN microfibers [35], with an aim of increasing the surface area. The surface of the electrospun PAN fibers was then reacted with a sodium hydroxide (NaOH) aqueous solution to introduce chemical

functionality that is capable of chelating metal ions. The functional groups of the resulting fibers were determined by Fourier-transform infrared spectroscopy (FT-IR). The ability to capture metal ions was then evaluated against Cu(II) ions, using atomic absorption spectroscopy (AAS), and the results were compared with the hydrolyzed PAN microfibers.

3.3 Experimental Details

3.3.1 Materials

Commercially-available PAN microfibers (diameters of individual fibers = 13.7 ± 2.7 μm, weight-average molecular weight ≈ 55,500 Da, weight composition of methyl acrylate comonomer =8.6%; Thai Acrylic Fibre, Co., Ltd., Thailand) were used to prepare PAN solution for further fabrication into ultrafine PAN fiber mats by electrospinning. Dimethylformamide (DMF, research grade of 99.98% purity; Labscan Asia Co., Ltd., Thailand) was used as the solvent. Sodium hydroxide (NaOH; Fisher Scientific, USA) aqueous solutions were used to modify the surface of the PAN fibrous materials. A stock solution of Cu(II) ions was prepared from cupric chloride dihydrate ($CuCl_2 \cdot 2H_2O$, 99% purity; Fluka, USA).

3.3.2 Electrospinning of PAN Fiber Mats

The spinning solution at 10 wt% was prepared by dissolving the as-received PAN microfibers in DMF under mechanical stirring for about 1 h at room temperature (25 ± 1 °C) [35, 36]. The as-prepared solution was then loaded into a standard 10-mL glass syringe. A 20-gauge, blunt-ended stainless steel needle (outer diameter = 0.91 mm) was used as the nozzle. Both the syringe and the needle were tilted about 45° from a horizontal baseline. A sheet of aluminum (Al) foil, wrapped around a rotating cylinder (width and outer diameters of the cylinder ≈ 15 cm and rotational speed ≈ 50 rpm), was used as the collecting device. A Gamma High-Voltage Research ES30P-5W DC power supply (USA) was used to charge the solution, by attaching the emitting electrode (+) to the nozzle and the grounding one to the collecting device. An electrical potential of 15 kV was applied across a distance of 20 cm between the tip of the needle and the outer surface of the collecting

device (i.e., collection distance, measured at a right angle to the surface of the collecting device). The electrospun PAN fiber mats (hereafter, ePAN fiber mats) were collected continuously for 48 h, resulting in the fiber mats of 125 ± 10 μm in thickness. Prior to further uses, these fiber mats were placed *in vacuo* at room temperature (25 ± 1 °C) to remove as much solvent from them as possible.

3.3.3 Preparation and Characterization of Hydrolyzed ePAN Fiber Mats and Hydrolyzed PAN Microfibers

The hydrolysis of all of the PAN fibrous materials was carried out based on the method of Deng et al. [27], with slight modification. Specifically, each of the ePAN fiber mat samples was placed in a sealed chamber, containing a NaOH solution in a mixed solvent of ethanol/water (at 0.22 molar ratio) of varying concentrations in the range of 1 to 5 wt%. The reaction time and the reaction temperature were fixed at 20 min and 75 °C, respectively. All of the reaction chambers were placed in a shaking water bath. The hydrolyzed ePAN fiber mats (hereafter, H-ePAN fiber mats) were washed with distilled water until of neutral pH and dried overnight *in vacuo* at room temperature (25 ± 1 °C). For comparison, hydrolyzed PAN microfibers were also prepared from the as-received PAN microfibers (hereafter, H-PAN fibers). The concentrations of the NaOH solution were 5, 7, and 10 wt% and the reaction times were 20, 40, and 60 min. The reaction temperature was, again, fixed at 75 °C.

Chemical functionalities of all of the fibers were characterized by a Nicolet Impact 400 Fourier-transform infrared spectroscope (FT-IR), operating at a resolution of 4 cm^{-1} and a wavenumber range of 4000 to 400 cm^{-1}. Morphologies of all of the fibers were investigated by a JEOL JSM-6400 scanning electron microscope (SEM). Each specimen was coated with a thin layer of gold using a JEOL JFC-1100E sputtering device prior to the SEM observation. The diameters of the individual microfibers were measured from 3500x SEM images and those of the individual electrospun fibers were from 10,000x ones, using a SemAphore 4.0 software. More than 10 and 50 individual fibers (for the microfibers and the electrospun fibers, respectively) were measured for their diameters. Ion exchange capacities (IEC) were used to quantify the contents of the as-formed imine groups of

the H-ePAN fiber mats and the H-PAN fibers. Briefly, each of the fiber samples (i.e., 0.1 g) was immersed in 25 mL of 0.1 M hydrochrolic acid (HCl) aqueous solution at 25 °C for 24 h. The amount of the excess acid in each of the supernatant liquids was determined by titration with 0.1 M NaOH aqueous solution [19].

Any interaction that occurred between the adsorbed Cu(II) ions and the chelating moieties on the surface of the H-ePAN fibers was analyzed by a Thermo Fisher Scientific Thetaprobe X-ray photoelectron spectroscope (XPS). Monochromatic Al Kα X-ray was employed for the analysis of one spot on each sample with a photoelectron take-off angle of 50° (with respect to the surface plane). The observation area was approximately 400 μm × 400 μm and the maximal analytical depth was in the range of about 4-8 nm. A specially-designed electron flood gun, capable of generating a few eV Ar+ ions, was used for the charge compensation. Electron and ion beams were focused and steered towards the observation area. Further correction was made based on adventitious C 1s at 285.0 eV, using the manufacturer's standard software. Survey spectra were acquired for surface composition analysis with Scofield sensitivity factors.

3.3.4 Adsorption of Cu(II) Ions on Fibrous Substrates

The adsorption of metal ions were studied by batch method. Each of the H-ePAN fiber mat and the H-PAN fiber samples (0.1 g) was placed in a bottle containing a 200 ppm Cu(II) ion solution. Each bottle was shaken in a shaking water bath at 100 rpm and a controlled temperature of 30 °C for 24 h. The adsorbed amounts (i.e., adsorption capacity, q in $mg \cdot g^{-1}$) of Cu(II) ions on both types of the fibrous substrates were determined from the initial and the final concentrations of the Cu(II) ions in the testing solutions, using a Varian SpectrAA-300 atomic absorption spectroscope (AAS). The effects of the pH, the contact time, and the initial metal ion concentration on the adsorption capacity of the APAN nanofiber mats were examined. Specifically, the values of q were determined from the following equation:

$$q = \frac{(C_0 - C_e)V}{M}, \qquad (1)$$

where C_0 and C_e are the initial and the equillibium Cu(II) ion concentrations ($mg \cdot L^{-1}$), V is the volume of the testing solution (L), and M is the initial, dry weight of the adsorbent (g)[4].

3.3.5 Desorption of Cu(II) Ions from Fibrous Substrates

The H-ePAN fiber mat and the H-PAN fiber samples (25 ± 1 mg), that had been pre-adsorbed with Cu(II) ions according to the procedure set-forth in Section 2.4.3 for 24 h (to exhibit the adsorbed amounts of Cu(II) ions of 0.67 ± 0.03 mg), were used in the desorption studies. First, they were rinsed with distilled water to remove any residual solution and were dried *in vacuo* at room temperature (25 ± 1 °C). The desorption behavior of the pre-adsorbed materials was carried out in deionized (DI) water or 0.1 or 1.0 M HCl aqueous solution. The contents of the flasks were shaken in the shaking water bath at 100 rpm and a controlled temperature of 30 °C. The Cu(II) ion concentrations in the desorbing solutions were analyzed as a function of submersion time by AAS. The desorption ratio (%*D*), for each data point, was calculated based on the percentage of the ratio between the desorbed and the initial, adsorbed amounts of Cu(II) ions.

3.4 Results and Discussions

3.4.1 Characterization of H-ePAN Fiber Mats and H-PAN Fibers

3.4.1.1 Visual Observation and FT-IR Analysis

The H-ePAN fiber mats were successfully synthesized from the ePAN fiber mats. The hydrolytic reaction was conducted at different concentrations of the NaOH solution (i.e., from 1 to 5 wt%). The color of the ePAN fiber mats was white. After the hydrolysis, the color of the mats changed to orange. Upon being washed with distilled water, the color of the mats changed further to light yellow. The shade the colors appeared deeper as the concentration of the NaOH solution changed from 1 to 5 wt%. Any change in the chemical functionalities of the H-ePAN fiber mats was analyzed by FT-IR. The corresponding spectra are shown in Figure 3.1. The intensity of the broad adsorption band at 3357 cm^{-1}, corresponding to the stretching vibration of O-H, increased with an increase in the basicity of the

treating solution. This indicates the introduction of the –OH groups on the surface of the H-ePAN fiber mats. Additionally, an increase in the basicity of the treating solution caused the intensities of three absorption peaks at 1578, 1404, and 1223 cm^{-1} to increase. These peaks can be assigned to imine conjugated sequences (-C=N-) of the modified fibers [27, 37]. Since only a fraction of the nitrile groups on the surface of the ePAN fibers was converted to the imine conjugated sequences, the peak at 2243 cm^{-1}, corresponding to the stretching vibration of the nitrile groups, decreased in its intensity with an increase in the NaOH concentration. Additionally, the intensity of the peak at 1739 cm^{-1}, corresponding to the stretching vibration of the carbonyl of the acrylate esters, became weaker, as the acrylate groups was converted to carboxylic groups upon hydrolysis. This is evidently characterized by the increase in the intensity of the peak at 1679 cm^{-1}, which corresponds to the stretching vibration of the carbonyl in the carboxylic groups. Based on the FT-IR results, the mechanism for the hydrolytic reaction of the ePAN fiber mats to obtain the H-ePAN fiber mats can be shown in Scheme 3.1.

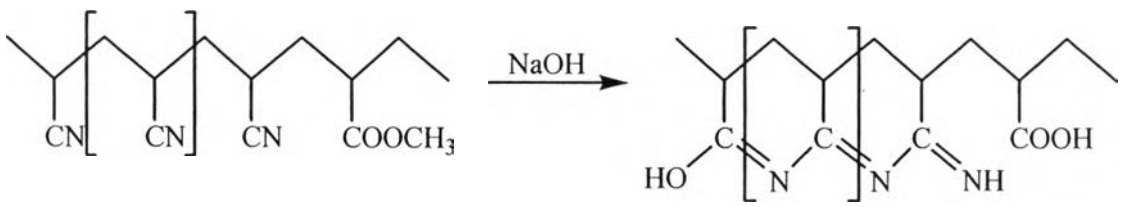

Scheme 3.1. Hydrolysis of ePAN fiber mats and PAN microfibers by NaOH aqueous solution into H-ePAN fiber mats and H-PAN fibers.

In case of the H-PAN fibers, the hydrolytic reaction was conducted at various NaOH solution concentrations (i.e., 5, 7, and 10 wt%) and reaction times (i.e., 20, 40, and 60 min). The change in the color from white of the neat PAN microfibers to orange and light yellow, respectively, of the H-PAN fibers was also observed. As in the case of the H-ePAN fiber mats, the shade of the colors appeared deeper with increases in both the concentration of the NaOH solution and the reaction time. The successful synthesis of H-PAN fibers was confirmed by FT-IR (see Figures I-III in Supplementary Data). Similar to the results for the H-ePAN fiber mats, the increases in both the NaOH concentration and the reaction time resulted in greater amounts of

imine conjugated sequences introduced on the H-PAN fiber surfaces. Since the diameters of the PAN microfibers were much greater than those of the ePAN fibers, much harsher hydrolytic conditions could be imposed on them than on the ePAN counterparts.

3.4.1.2 Ion Exchange Capacities

Ion exchange capacities (IEC) of both the H-ePAN fiber mats and the H-PAN fibers were investigated. Figure 3.2a shows the number of the exchange sites available to protons for each of the H-ePAN fiber mats that had been synthesized at different concentrations of the NaOH solution. As the conversion of the nitrile groups to the imine conjugated sequences increased with an increase in the NaOH concentration, the number of the available exchange sites also increased. As evidently shown by FT-IR (see Figure 3.1), the hydrolytic treatment of the ePAN fiber mats with the NaOH solution introduced both –OH and –COOH groups on the surfaces of the H-ePAN fibers (see Scheme 3.1), causing them to be more hydrophilic. This, in turn, caused the fiber mats that had been treated with the NaOH solution at the concentrations greater than 3 wt% to become gel-like matrices (see results in Section 3.4.1.3), which could be a direct result of the increase in the swelling in an aqueous medium of the treated membranes [27,37]. The number of the exchange sites available to protons for each of the H-PAN fibers that had been synthesized at different hydrolytic conditions is also shown in Figure 3.2b. Generally, increases in both the NaOH concentration and the reaction time caused the number of the available exchange sites to increase. Interestingly, at the same hydrolytic condition for both type of the fibrous substrates (i.e., 5 wt% NaOH solution for 20 min), the IEC of the H-ePAN fiber mats was about 7 times greater than that of the H-PAN fibers. This should be a direct result of the much smaller diameters of the ePAN fibers, hence the greater specific surface area.

3.4.1.3 SEM Observation

Figure 3.3 shows representative SEM images of the ePAN and the H-ePAN fiber mats. The individual fibers of the ePAN fiber mats were cross-sectionally round and their surfaces were smooth [35]. After having been hydrolyzed with 1-3 wt% NaOH solutions, the fiber mats shrank considerably, as the thicknesses of the fiber mats and the diameters of the individual fibers decreased monotonically

from 125 ± 10 μm and 280 ± 80 nm for the ePAN fiber mats to 101 ± 10 μm and 245 ± 60 nm for the ones that had been treated with 1 wt% NaOH solution to 92 ± 10 μm and 225 ± 60 nm for the ones that had been treated with 2 wt% NaOH solution and, finally, to 87 ± 10 μm and 195 ± 60 nm for the ones that had been treated with 3 wt% NaOH solution. Nevertheless, the fibrous character of these H-ePAN fiber mats was still retained. Upon further treatment with 4 and 5 wt% NaOH solutions, the shrinkage became so severe that the individual fibers fused together at touching points. This should be due to the presence of both –OH and –COOH groups introduced on the surfaces of the H-ePAN fibers as a result of the hydrolytic treatment. Figure 3.4 shows representative SEM images of the PAN and the H-PAN microfibers. Evidently, harsher conditions used in the hydrolytic treatment of the PAN fibers as compared to those of the ePAN fiber mats resulted in the erosion of the surfaces of the obtained H-PAN fibers. This indicates that the hydrolytic reaction occurred merely on the surface of the PAN fibers, hence the observed increase in the surface roughness [22, 27]. In analogy to that observed for the ePAN and the H-ePAN fibers, the diameters of the H-PAN fibers also decreased from those of the PAN microfibers, upon the hydrolytic treatment with the NaOH solutions, and the values decreased monotonically with increases in both the NaOH concentration and the time upon which the fibers had been treated.

Based on the morphologies of the obtained H-ePAN fiber mats and H-PAN fibers, the ones that had been obtained from the treatment with 3 wt% NaOH solution (for the H-ePAN fiber mats) and 10 wt% NaOH solution for 40 min (for the H-PAN fibers) were chosen for subsequent adsorption studies. By referring to the IEC results in Section 3.1.2, these materials exhibited the IEC values of 0.86 ± 0.02 and 1.04 ± 0.01 $mmol \cdot g^{-1}$, respectively.

3.4.2 Adsorption of Cu(II) Ions on Fibrous Substrates

3.4.2.1 Effect of Initial pH

The adsorption of Cu(II) ions on the H-ePAN fiber mat and H-PAN fiber samples was first investigated as a function of the initial pH of the 200 ppm Cu(II) ion solution. The initial pH of the testing solutions was varied in the range of 2.0 to 7.0 by the addition of either 0.1 M HCl or 0.1 M NaOH aqueous

solution. To avoid the precipitation of metal ions, no adsorption experiments were done at a pH greater than 7. It should be noted that, after adsorption, the color of the fibrous substrates changed from light yellow to pale blue (i.e., the color of the Cu(II) ion solution) and that the contact time of 24 h was ample for the adsorption of Cu(II) ions to reach an equilibrium (see results in Section 3.4.2.3). At low pH's (i.e., 2.0 and 3.0), the average, adsorbed amounts of Cu(II) ions on both types of the fibrous substrates were low (i.e., about 2 $mg \cdot g^{-1}$ for the H-ePAN fiber mats and about 0.5-0.6 $mg \cdot g^{-1}$ for the H-PAN fibers). This should be due to the competitive adsorption between the prevalently-available H^+ and the Cu(II) ions. The electrostatic repulsion between the protonated imine groups of the modified fibrous matrices and Cu(II) ions could be another reason for the very low adsorption values [37]. Marked increase in the adsorbed amounts of Cu(II) ions was observed when the initial pH of the Cu(II) ion solution increased further from 3.0 to 5.0. At the pH of 5.0, the adsorbed amounts of Cu(II) ions on the H-ePAN fiber mats were 25.5 ± 0.1 $mg \cdot g^{-1}$, while those on the H-PAN fibers were slightly greater at 28.2 ± 0.5 $mg \cdot g^{-1}$. The decrease in the amounts of H^+, due to the increase in the initial pH, resulted in less competitive adsorption on the available adsorptive sites as well as in the increase in the number of available adsorptive sites because of the decrease in the probability of the imine groups on the H-ePAN fiber mats become protonated. Further increase in the initial pH of the Cu(II) ion solution only resulted in a slight increase in the average, adsorbed amounts of Cu(II) ions on both substrates (i.e., about 26.1 $mg \cdot g^{-1}$ for the H-ePAN fiber mats and about 31.5 $mg \cdot g^{-1}$ for the H-PAN fibers, at pH 7.0). Based on the obtained results, the pH of 5.0 was chosen as the initial pH of the Cu(II) ion solution for subsequent studies and the reason for the greater adsorption of Cu(II) ions on the H-PAN fibers was due to the harsher hydrolytic condition to obtain the materials, which caused the H-PAN fibers to exhibit greater IEC values, despite the hypothetical lower specific surface area.

3.4.2.2 Adsorption Isotherms

The effect of the initial concentration (C_0) of the Cu(II) ions in the testing solutions on the adsorbed amounts of them on both types of the fibrous materials was investigated by varying initial concentrations (40–800 ppm) of Cu(II)

solutions with the initial pH of 5.0 and the results are reported in Figure 3.5 as the functions of the equilibrium adsorption capacity of Cu(II) ions (q_e) versus the equilibrium concentration of Cu(II) ions in the testing solutions (C_e). For each type of the fibrous matrices, q_e increased very rapidly with an initial increase in C_e and reached a plateau value as C_e increased further. Mathematically, the adsorption data can be analyzed based on Langmuir and Freundlich models [27, 38]. The Langmuir model was developed to describe the adsorption of an adsorbate on a homogenous, flat surface of an adsorbent. The model assumes that each adsorptive site can only be occupied once in a one-on-one manner. Mathematically, the model can be written as follows [27, 38]:

$$\frac{C_e}{q_e} = \frac{C_e}{q_m} + \frac{1}{K_L q_m}, \tag{2}$$

where q_m is the maximal adsorption capacity of the metal ions on the adsorbent ($mg \cdot g^{-1}$) and K_L is the adsorption equilibrium constant ($mL \cdot mg^{-1}$). The value of q_m is taken as the slope of the plot of C_e/q_e versus C_e, while that of K_L can be calculated from the values of the slope and the y-intercept of the plot (i.e., slope/y-intercept). The Freundlich model, on the other hand, is used to describe the adsorption of an absorbate on a heterogeneous surface of an adsorbent. The mathematical expression of this model can be written as follows [4, 7]:

$$q_e = K_F C_e^{1/n}, \tag{3}$$

where K_F [$mg^{(1-1/n)} \cdot L^{1/n} \cdot g^{-1}$] and n are Freundlich constants. By plotting log q_e as a function of log C_e, the value of K_F is taken as the anti-logarithmic value of the y-intercept and n is the inverse value of the slope.

The adsorption data, as reported in Figure 3.5, were analyzed according to these models and the results are summarized in Table 3.1. Evidently, both data sets were fitted particularly well with the Langmuir model, as the values of the correlation coefficient (r^2) were extremely high (i.e., 0.9999). The value of q_m for the H-ePAN fiber mats was about 31 $mg \cdot g^{-1}$, while that for the H-PAN fibers was slightly greater at about 36 $mg \cdot g^{-1}$. The much harsher hydrolytic condition levied on

the more robust PAN microfibers, hence the greater IEC value, was obviously responsible for the greater adsorption of Cu(II) ions onto the H-PAN fibers, despite the hypothetical greater specific surface area of the H-ePAN fibers. Compared with some of the literature data, the values of q_m for both of the H-ePAN and the H-PAN fibrous substrates as obtained in the present study were comparable to those reported for amidoximated bagasse (27.6 $mg \cdot g^{-1}$) [7], aminated PAN microfibers (31.5 $mg \cdot g^{-1}$) [22] and hydrolyzed PAN microfibers (29.6 $mg \cdot g^{-1}$) [27]. On the other hand, they were lower than those reported for the polyacrylamidoxime microfibers (71.1 $mg \cdot g^{-1}$) [18], polyacrylamidoxime electrospun fibers (52.7 $mg \cdot g^{-1}$) [34] and poly(acryloamidino diethylenediamine) microfibers (285 $mg \cdot g^{-1}$) [24]. Due to the expensiveness of the chemical reagents and the complexity of the chemical reaction for both polyacrylamidoxime and poly(acryloamidino diethylenediamine), hydrolyzed PAN seems to have an edge for actual industrial utilization.

3.4.2.3 Effect of Contact Time

The adsorption of the Cu(II) ions on any type of the fibrous substrates increased rapidly with an initial increase in the contact time (i.e., high adsorption rate) to finally reach the maximal, plateau value after the substrate had been in contact with the Cu(II) ion solution for about 5 h. For the ePAN fiber mats, the maximal adsorbed amounts of Cu(II) ions were 2.1 ± 0.5 $mg \cdot g^{-1}$ (at 24 h), while, for the PAN microfibers, they were 1.4 ± 0.7 $mg \cdot g^{-1}$ (at 24 h). The low adsorption of Cu(II) ions on these substrates should be a result of the weak interaction between Cu(II) ions and the lone-pair nitrogen electrons of the nitrile groups on the surface of the fibers. On the contrary, much greater amounts of Cu(II) ions could be adsorbed onto the surfaces of the hydrolyzed fibrous materials, which is apparently a result of the presence of the imine conjugated sequences [27, 37, 38]. Evidently for both types of the hydrolyzed fibrous matrices, the adsorption of Cu(II) ions onto their surfaces occurred in two steps. Initially, the adsorption was swift because of the great number of free adsorptive sites and the high concentration of the metal ions. In the second step, adsorption rates decreased and finally reached equilibria. This results from the depletion of the adsorptive sites and the decreased Cu(II) ion concentration in the testing solution. At 24 h of submersion, the maximal adsorbed amounts of Cu(II)

ions on the H-ePAN fiber mats were 29.2 ± 0.8 $mg \cdot g^{-1}$, while those on the H-PAN fibers were 34.3 ± 0.9 $mg \cdot g^{-1}$.

3.4.2.4 Kinetic of Cu(II) Adsorption

The kinetics of Cu(II) ion adsorption on the H-ePAN fiber mats and the H-PAN fibers were analyzed using pseudo-first-order and pseudo-second-order models. The pseudo-first-order kinetic model is widely used to describe the adsorption of solid/liquid systems, which assumes that the adsorption rate is related to the amount of unoccupied sites. The model is represented mathematically as follows [4, 7]:

$$\log(q_e - q_t) = \log q_e - \frac{k_1}{2.303} t, \quad (4)$$

where q_t stands for the adsorption capacity of the metal ions at an arbitrary time t (mg g^{-1}) and k_1 is the pseudo-first-order rate constant (mg g^{-1} min^{-1}). By plotting $\log(q_e - q_t)$ as a function of the contact time t (Figure 3.6a), the values of the calculated q_e (i.e., $q_{e,cal}$) and the rate constant k_1 can be obtained from the antilogarithmic value of the y-intercept and the slope of the plot, respectively. The values of k_1 and $q_{e,cal}$ along with those of the correlation coefficient (r^2) are summarized in Table 3.2.

The pseudo-second-order kinetic model, on the other hand, is derived based on the notion that the adsorption should relate to the squared product of the difference between the number of the equilibrium adsorptive sites available on an adsorbent and that of the occupied sites. The final mathematical representation of this model is given as [4, 7]:

$$\frac{t}{q_t} = \frac{1}{k_2 q_e^2} + \frac{t}{q_e}, \quad (5)$$

where k_2 is the pseudo-second-order rate constant (g mg^{-1} min^{-1}). Through the construction of the linear plots between t/q_t as a function of the contact time t (Figure 3.6b), the values of the calculated q_e (i.e., $q_{e,cal}$) and the rate

constant k_2 can be obtained from the inverse values of the slope and the y-interception values, respectively. The values of k_2 and $q_{e,cal}$ along with those of the correlation coefficient (r^2) are also summarized in Table 3.2.

Based on the values of the correlation coefficient (r^2), it can be conclude that the adsorption of Cu(II) ions on both types of the fibrous materials was better described with the pseudo-second-order model. Interestingly, the $q_{e,cal}$ values as obtained from the pseudo-second-order equation were in good agreement with the q_e values obtained from the experiment (i.e., $q_{e,exp}$). Similar conclusion was also reported for the adsorption of Cu(II) ions on various adsorbent [39–41].

3.4.2.5 XPS Studies

XPS was used to investigate electronic properties of a H-ePAN fiber mat both before and after the adsorption study in 200 ppm Cu(II) ion solution at pH 5.0 for 24 h. Figure 3.7a shows the N 1*s* spectrum of the H-ePAN fiber mat. Since the binding energies of imine and nitrile groups were found to be in the same region (i.e., 398.4–399.8 eV versus 398.7–399.4 eV) [42], the peak centering at 399.4 eV could be assigned to the N 1*s* core-level spectrum of N-atoms associated with the imine conjugated sequences [27]. Additionally, the peaks centering at 400.1 and 401.3 eV could be assigned to the C-N bonding and the protonated imines [43, 44], respectively. After the adsorption study, two deconvoluted peaks, centering at 398.4 and 399.9 eV, could be observed (see Figure 3.7b). The presence of these peaks suggested that the adsorbed Cu(II) ions altered the electronic properties of the bound N-atoms associated with the imine conjugated sequences, causing the electrons to locate closer to the ions and, hence, increasing the N 1*s* binding energy. Figure 3.7c shows the Cu $2p_{3/2}$ core-level spectrum of the H-ePAN fiber mat after the copper adsorption study. Two deconvoluted peaks centering at 931.9 and 933.5 eV could be assigned to Cu(I)/Cu(0) and Cu(II), respectively [27, 43–45]. The result suggested that, after the adsorption, some of the Cu(II) ions formed tight bonding with the N-atoms of the imine groups, causing their electron cloud densities to increase, hence the observed decrease in the binding energy [27]. Finally, O 1*s* spectrum of the H-ePAN fiber mat after the copper adsorption study could be deconvoluted into two peaks, centering at 530.5 and 532.3

eV (see Figure 3.7d). While the first peak could be assigned to the –OH groups that were formed onto the surface fibers after the hydrolysis (see Scheme 1) [27], the presence of the latter peak suggested that some of the Cu(II) ions interacted with the O-atoms of these –OH groups, drawing electrons closer to them and, hence, increasing the O 1*s* binding energy.

3.4.3 Desorption of Cu(II) Ions from Fibrous Substrates

Desorption of Cu(II) ions from the surface of the H-ePAN fiber mats was carried out in DI water or 0.1 M HCl aqueous solution, while that from the surface of the H-PAN fibers was carried out in DI water or 0.1 or 1.0 M HCl aqueous solution. The desorption ratio (%*D*) increased rapidly with an initial increase in the submersion time (i.e., high desorption rate) to finally reach the maximal, plateau value after the substrates had been submerged in the desorbing solution for at least about 30 min. In DI water, the maximal amounts of the Cu(II) ions desorbed from the H-ePAN fiber mats and the H-PAN fibers were practically similar, with the values being 4.2 ± 0.3 and 4.1 ± 0.3%, respectively. On the other hand, 98.9 ± 1.3% of the adsorbed Cu(II) ions was released from the H-ePAN fiber mats upon their submersion in 0.1 M HCl aqueous solution, while much lower values were obtained for the H-PAN fibers (i.e., 80.1 ± 0.8%). To achieve a similar desorption level to that obtained on the H-ePAN fiber mats, the concentration of the HCl aqueous solution used in the desorption of the H-PAN fibers needed to be at least 1.0 M, at which condition, the %*D* of 98.1 ± 1.7% could be achieved. It should be noted that these reported values were obtained at 60 min of submersion in the desorbing solutions.

3.5 Conclusions

The H-ePAN fiber mats were obtained from the hydrolytic treatment of the ePAN fiber mats using a NaOH solution. The conversion of the nitrile groups, native to PAN, into the imine conjugated sequences could be identified simply from the change in the color from whitish of the ePAN fiber mats to light yellowish of the post-washed H-ePAN fiber mats. Chemically, this was confirmed by FT-IR. The extent of the conversion increased with an increase in the concentration of the NaOH solution. The chelating property of the H-ePAN fiber mats was evaluated using

Cu(II) ions as the model hazardous metal ions. The initial pH of the Cu(II) ion solution posed a strong influence on the adsorption behavior of the H-ePAN fiber mats, with the initial pH of 5.0 being the optimal condition. The adsorption capacity of the H-ePAN fiber mats towards the Cu(II) ions increased with an increase in the time interval the materials were in contact with the Cu(II) ion solution and the equilibrium was reached after about 5 h of immersion. The isotherm for the adsorption of Cu(II) ions on the H-ePAN fiber mats was studied and was fitted well to the Langmuir equation, with the maximal adsorption capacity being 31.3 $mg \cdot g^{-1}$. Lastly, desorption of the pre-adsorbed H-ePAN fiber mats was achieved upon their submersion in 0.1 M HCl aqueous solution for at least 30 min.

3.6 Acknowledgments

The authors acknowledged partial support received from (a) the Petroleum and Petrochemical College (PPC, Chulalongkorn University) and (b) the Center for Petroleum, Petrochemicals, and Advanced Materials (CPPAM, Chulalongkorn University). PK is grateful for a doctoral scholarship received from the Royal Golden Jubilee PhD Program (PHD/0164/2550), the Thailand Research Fund (TRF).

3.7 References

[1] Immamuglu, M.; Tekir, O. Removal of copper (II) and lead (II) ions from aqueous solutions by adsorption on activated carbon from a new precursor hazelnut husks. Desalination 2008, 228, 108–113.

[2] Ren, Y. M.; Zhang, M. L.; Zhao, D. Synthesis and properties of magnetic Cu (II) ion imprinted composite adsorbent for selective removal of copper. Desalination 2008, 228, 135–149.

[3] Rengaraj, S.; Yeon, J. W.; Kim, Y.; Jung, Y.; Ha, Y. K.; Kim, W. H. Adsorption characteristics of Cu(II) onto ion exchange resins 252H and 1500H: Kinetics, isotherms and error analysis. J. Hazard. Mater. 2007,143, 469–477.

[4] Aman, T.; Kazi, A. A.; Sabri, M. U.; Bano, Q. Potato peels as solid waste for the removal of heavy metal copper(II) from waste water industrial effluent. Colloid Surf., B 2008, 63, 116–121.

[5] The Pollution Control Department of the Ministry of Natural Resources and Environment of Thailand. Provisional Guidelines Controlling the Quality of Wastewater from Industries and Industrial Villages; The 3rd Announcement of the Ministry; 1996 (in Thai).

[6] World Health Organization (WHO). Copper in Drinking-Water: Background Document for Development of WHO Guidelines for Drinking-Water Quality; 2004.

[7] Jiang, Y.; Pang, H.; Liao, B. Removal of copper(II) ions from aqueous solution by modified bagasse. J. Hazard. Mater. 2009, 164, 1–9.

[8] Aydin, A.; Imamoglu, M.; G€ulfen, M. Separation and recovery of gold(III) from base metal ions using melamine formaldehyde thiourea chelating resin. J. Appl. Polym. Sci. 2008, 107, 1201–1206.

[9] Mauchauffe, S.; Meux, E. Use of sodium decanoate for selective precipitation of metals contained in industrial wastewater. Chemosphere 2007, 69, 763–768.

[10] Mohandas, J.; Kumara, T.; Rajan, S. K.; Velmurugan, S.; Narasimhan, S. V. Introduction of bifunctionality into the phosphinic acid ion-exchange resin for enhancing metal ion complexation. Desalination 2008, 232, 3–10.

[11] Rangel-Mendeza, J. R.; Monroy-Zepedab, R.; Leyva-Ramosb, E.; Diaz-Floresa, P. E.; Shirai, K. Chitosan selectivity for removing cadmium (II), copper (II), and lead (II) from aqueous phase: pH and organic matter effect. J. Hazard. Mater. 2009, 162, 503–511.

[12] Ko, Y. G.; Choi, U. S. Observation of metal ions adsorption on novel polymeric chelating fiber and activated carbon fiber. Sep. Purif. Technol. 2007, 57, 338–347.

[13] Mugisidi, D.; Ranaldo, A.; Soedarsono, J. W.; Hikam, M. Modification of activated carbon using sodium acetate and its regeneration using sodium hydroxide for the adsorption of copper from aqueous solution. Carbon 2007, 45, 1081–1084.

[14] Gong, B.; Li, X.; Wang, F.; Chang, X. Synthesis of spherical macroporous epoxy-dicyandiamide chelating resin and properties of concentration and separation of trace metal ions from samples. Talanta 2000, 52, 217–223.

[15] Chen, C. Y.; Lin, M. S.; Hsu, K. R. Recovery of Cu(II) and Cd(II) by a chelating resin containing aspartate groups. J. Hazard. Mater. 2008, 152, 986–993.

[16] Liu, R.; Tang, H.; Zhang, B. Removal of Cu(II), Zn(II), Cd(II) and Hg(II) from waste water by poly(acrylaminophosphonic)-type chelating fiber. Chemosphere 1999, 38, 3169–3179.

[17] Sun, S.; Wang, A. Adsorption properties of N-succinyl-chitosan and cross-linked N-succinyl-chitosan resin with Pb (II) as template ions. Sep. Purif. Technol. 2006, 51, 409–415.

[18] McComb, M. E.; Gesser, H. D. Preparation of polyacryloamidoxime chelating cloth for the extraction of heavy metals from water. J. Appl. Polym. Sci. 1997, 65, 1175–1192.

[19] Bilba, N.; Bilba, D.; Moroi, G. Synthesis of a polyacrylamidoxime chelating fiber and its efficiency in the retention of palladium Ions. J. Appl. Polym. Sci. 2004, 92, 3730–3735.

[20] Kozody_nska, D. Iminodisuccinic acid as a new complexing agent for removal of heavy metal ions from industrial effluents. Chem. Eng. J. 2009, 152, 277–288.

[21] Gong, B. Synthesis of polyacrylaminoimidazole chelating fiber and properties of concentration and separation of trace Au, Hg and Pd from samples. Talanta 2002, 57, 89–95.

[22] Deng, S.; Bai, R.; Chen, J. P. Aminated polyacrylonitrile fibers for lead and copper removal. Langmuir 2003, 19, 5058–5064.

[23] Miretzky, P.; Cirelli, A. F. Hg(II) removal from water by chitosan and chitosan derivatives: A review. J. Hazard. Mater. 2009, 167, 10–23.

[24] Ko, Y. G.; Choi, U. S.; Park, Y. S.; Woo, J. W. Fourier-transform infrared spectroscopy study of the effect of pH on anion and cation adsorption onto poly(acryloamidino diethylenediamine). J. Polym. Sci., Polym. Chem. 2004, 42, 2010–2018.

[25] Gong, B.; Li, X.; Wang, F.; Xua, H.; Chang, X. Synthesis of polyacrylacylaminourea chelating fiber and properties of concentration and separation of trace metal ions from samples. Anal. Chim. Acta 2001, 427, 287–291.

[26] Chang, X.; Yang, X.; Wei, X.; Wu, K. Efficiency and mechanism of new poly(acryl-phenylamidrazone phenylhydrazide) chelating fiber for adsorbing trace Ga, In, Bi, V and Ti from solution. Anal. Chim. Acta 2001, 450, 231–238.

[27] Deng, S.; Bai, R.; Chen, J. P. Behaviors and mechanisms of copper adsorption on hydrolyzed polyacrylonitrile fibers. J. Colloid Interface Sci. 2003, 260, 265–272.

[28] Reneker, D. H.; Yarin, A. L. Electrospinning jets and polymernanofibers. Polymer 2008, 49, 2387–2425.

[29] Shin, Y. M.; Hohman, M. M.; Brenner, M. P.; Rutledge, G. C. Experimental characterization of electrospinning: the electrically forced jet and instabilities. Polymer 2001, 42, 9955–9967.

[30] Supaphol, P.; Chuangchote, S. On the electrospinning of poly(vinyl alcohol) nanofiber mats: a revisit. J. Appl. Polym. Sci. 2008, 108, 969–978.

[31] Wutticharoenmongkol, P.; Pavasant, P.; Supaphol, P. Osteoblastic phenotype expression of MC3T3-E1 cultured on electrospun polycaprolactone fiber mats filled with hydroxyapatite nanoparticles. Biomacromolecules 2007, 8, 2602–2610.

[32] Luu, Y. K.; Kim, K.; Hsiao, B. S.; Chu, B.; Hadjiargyrou, M. Development of a nanostructured DNA delivery scaffold via electrospinning of PLGA and PLA-PEG block copolymers. J. Controlled Release 2003, 89, 341–353.

[33] Taepaiboon, P.; Rungsardthong, U.; Supaphol, P. Drugloaded electrospun mats of poly(vinyl alcohol) fibres and their release characteristics of four model drugs. Nanotechnology 2006, 17, 2317–2329.

[34] Saeed, K.; Haider, S.; Oh, T.; Park, S. Preparation of amidoxime-modified polyacrylonitrile (PAN-oxime) nanofibers and their applications to metal ions adsorption. J. Membr. Sci. 2008, 322, 400–405.

[35] Sutasinpromprae, J.; Jitjaicham, S.; Nithitanakul,M.;Meechaisue, C.; Supaphol, P. Preparation and characterization of ultrafine electrospun polyacrylonitrile fibers and their subsequent pyrolysis to carbon fibers. Polym. Int. 2006, 55, 825–833.

[36] Kampalanonwat, P.; Supaphol, P. Preparation and adsorption behavior of aminated electrospun polyacrylonitrile nanofiber mats for heavy metal ion removal. ACS Appl. Mater. Inter. 2010, 2, 3619–3627.

[37] Karpacheva, G. P.; Zemtsov, L. M.; Bondarenko, G. N.; Litmanovich, A. D.; Plat_e, N. A. Formation of conjugated CdN bonds and their transformation in the alkaline hydrolysis of poly(acrylonitrile). Polym. Sci. Ser. A+ 2000, 42, 620–625.

[38] Bilba, D.; Suteu, D.; Malutan, T. Removal of reactive dye brilliant red HE-3B from aqueous solutions by hydrolyzed polyacrylonitrile fibres: equilibrium and kinetics modeling. Cent. Eur. J. Chem. 2008, 6, 258–266.

[39] Jing, X.; Liu, F.; Yang, X.; Ling, P.; Li, L.; Long, C.; Li, A. Adsorption performances and mechanisms of the newly synthesized N, N0-di(carboxymethyl) dithiocarbamate chelating resin toward divalent heavy metal ions from aqueous media. J. Hazard. Mater. 2009, 167, 589–596.

[40] Wang, X.; Zheng, Y.; Wang, A. Fast removal of copper ions from aqueous solution by chitosan-g-poly(acrylic acid)/attapulgite composites. J. Hazard. Mater. 2009, 168, 970–977.

[41] Shen, W.; Chen, S.; Shi, S.; Li, X.; Zhang, X.; Hu, W.; Wang, H. Adsorption of Cu(II) and Pb(II) onto diethylenetriamine-bacterial cellulose. Carbohydr. Polym. 2009, 75, 110–114.

[42] Pels, J. R.; Kapteijn, F.; Moulun, J. A.; Zhu, Q.; Thomas, K. M. Evolution of nitrogen functionalities in carbonaceous materials during pyrolysis. Carbon 1995, 33, 1641–1653.

[43] Dambies, L.; Guimon, C.; Yiacoumi, S.; Guibal, E. Characterization of metal ion interactions with chitosan by X-ray photoelectron spectroscopy. Colloids Surf., A 2001, 177, 203–214.

[44] Mosser, C.; Mosser, A.; Romeo, M.; Petit, S.; Decarreau, A. Natural and synthetic copper phyllosilicates studied by XPS. Clays Clay Miner. 1992, 40, 593–599.

[45] Martínez, J. M. L.; Rodríguez-Castellón, E.; Sánchez, R. M. T.; Denaday, L. R.; Buldaina, G. Y.; Dall' Orto, V. C. XPS studies on the Cu(I,II)-polyampholyte heterogeneous catalyst: An insight into its structure and mechanism. J. Mol. Catal. A: Chem. 2011, 339, 43–51.

Table 3.1 Values of the Parameters Associated with the Langmuir and the Freundlich Models, Including Those of the Correlation Coefficient, for the Adsorption of Cu(II) Ions onto the H-ePAN Fiber Mat and H-PAN Microfibers.

Adsorbent	Langmuir model			Freundlich model		
	q_m (mg g^{-1})	K_L (mL mg^{-1})	r^2	K_F ($mg^{(1-1/n)}$ $L^{1/n}$ g^{-1})	n	r^2
H-ePAN fiber mat	31.25	0.36	0.9999	13.43	2.66	0.9644
H-PAN fibers	35.71	0.12	0.9999	22.42	17.04	0.6189

Table 3.2 Kinetics Parameters Describing the Adsorption of Cu(II) Ions onto the H-ePAN fiber mat and the H-PAN fibers (see Results in Figure 7), Based on the Pseudo-First- and the Pseudo-Second-Order Kinetic Models.

Metal ions		Pseudo-first order			Pseudo-second order		
	$q_{e,exp}$ (mg g^{-1})	k_1 (mg g^{-1} min^{-1})	$q_{e,cal}$ (mg g^{-1})	r^2	k_2 (g mg^{-1} min^{-1})	$q_{e,cal}$ (mg g^{-1})	r^2
H-ePAN fiber mat	29.20	0.0295	9.89	0.9181	0.0140	29.26	0.9999
H-PAN fibers	34.30	0.0296	25.06	0.8475	0.0032	34.53	0.9999

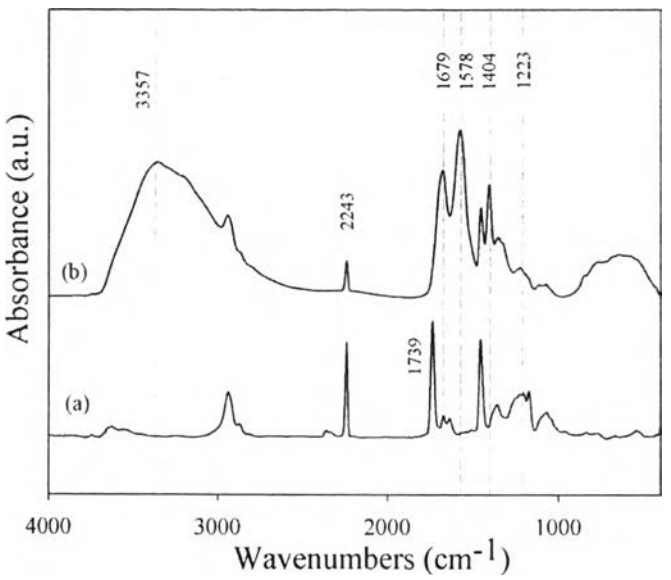

Figure 3.1 FT-IR spectra of (a) electrospun PAN fiber mats (hereafter, ePAN fiber mats) and (b) hydrolyzed electrospun PAN fiber mats (hereafter, H-ePAN fiber mats) that had been obtained from the reaction between the ePAN fiber mats and NaOH aqueous solution of 4, wt%.

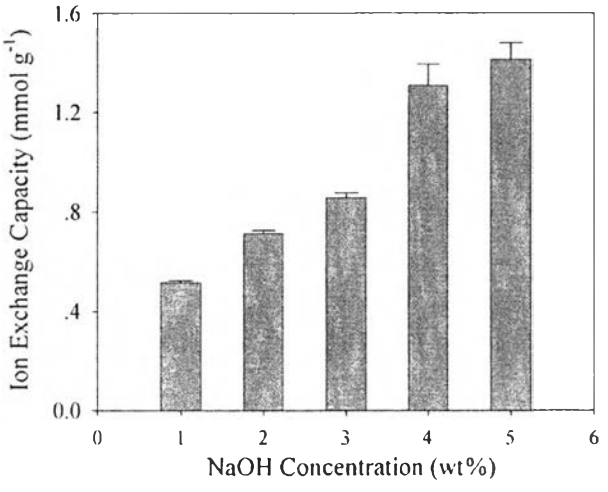

(a)

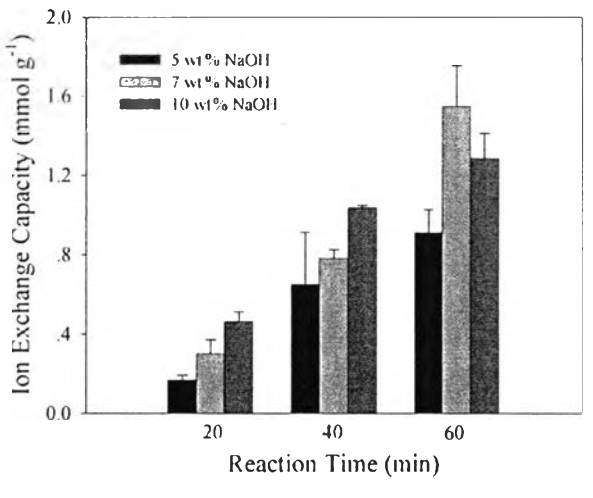

(b)

Figure 3.2 Ion exchange capacities of (a) H-ePAN fiber mats that had been synthesized at various NaOH aqueous solution concentrations and (b) H-PAN fibers that had been synthesized at various NaOH aqueous solution concentrations and reaction times.

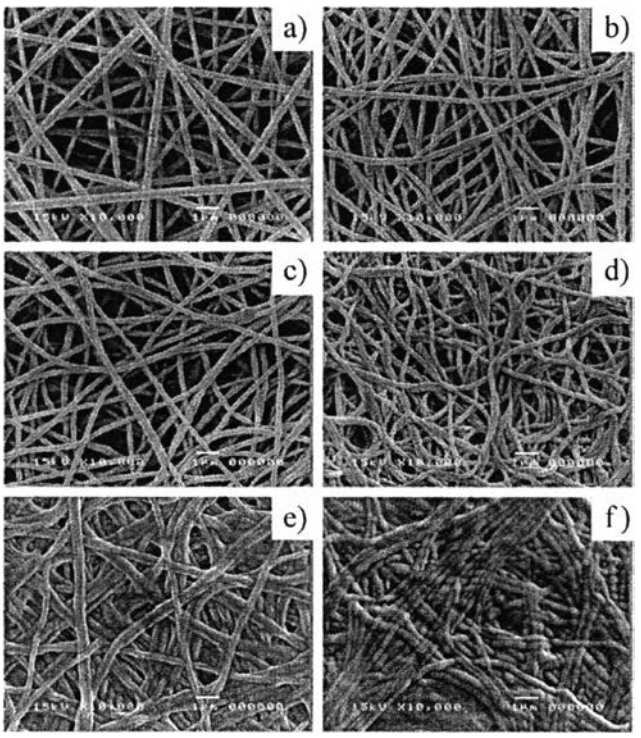

Figure 3.3 Representative SEM images of (a) ePAN fiber mat and H-ePAN fiber mats that had been obtained from the reaction of ePAN fiber mats with NaOH aqueous solution of varying concentrations: (b) 1, (c) 2, (d) 3, (e) 4, and (f) 5 wt%. Only the diameters of the ePAN fibers and the H-ePAN fibers that had been obtained upon the treatment with 1-3 wt% NaOH aqueous solutions could be measured, i.e., 280 ± 80, 245 ± 60, 225 ± 60, and 195 ± 60 nm, respectively.

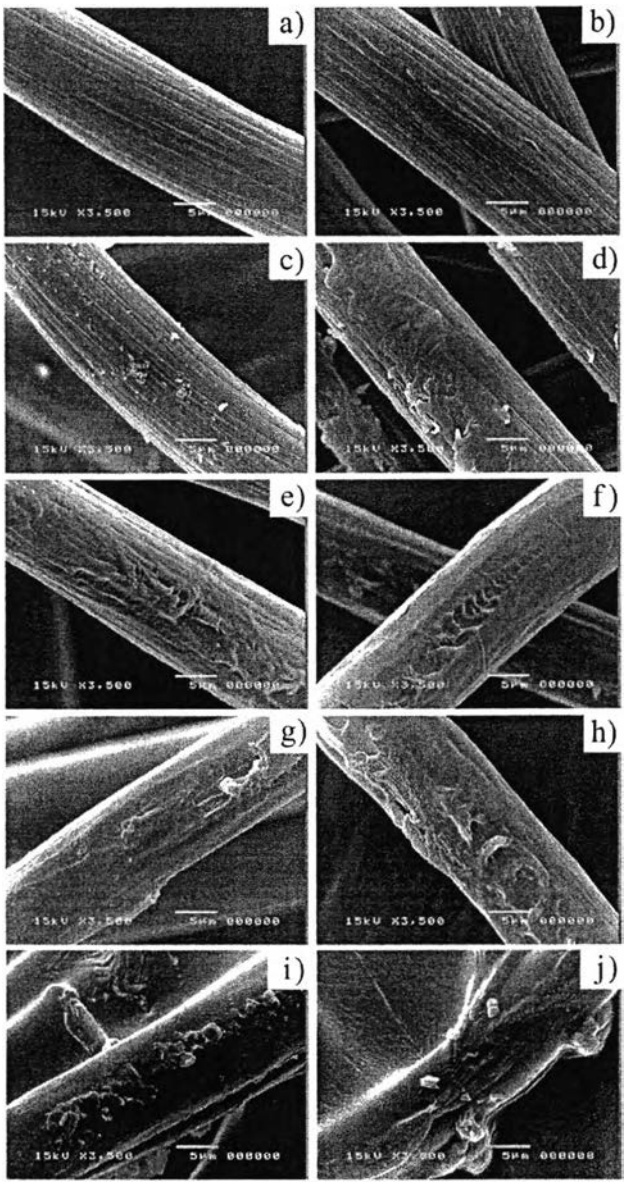

Figure 3.4 Representative SEM images (with fiber diameters being reported in parentheses) of (a) PAN microfibers (13.73 ± 2.70 μm) and H-PAN fibers that had been obtained from the reaction of PAN microfibers with NaOH aqueous solution of varying reaction conditions (NaOH concentration/reaction time): (b) 5 wt%/20 min (13.70 ± 2.63 μm), (c) 5 wt%/40 min (13.64 ± 3.39 μm), (d) 5 wt%/60 min (13.56 ± 3.86 μm), (e) 7 wt%/20 min (13.64 ± 5.07 μm), (f) 7 wt%/40 min (13.60 ± 1.99 μm), (g) 7 wt%/60 min (12.94 ± 2.94 μm), (h) 10 wt%/20 min (13.63 ± 3.34 μm), (i) 10 wt%/40 min (13.20 ± 3.18 μm), and (j) 10 wt%/60 min (12.90 ± 2.38 μm).

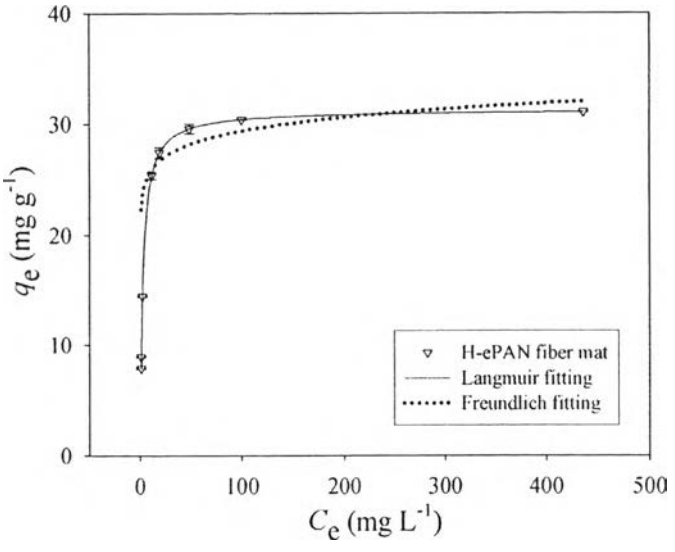

(a)

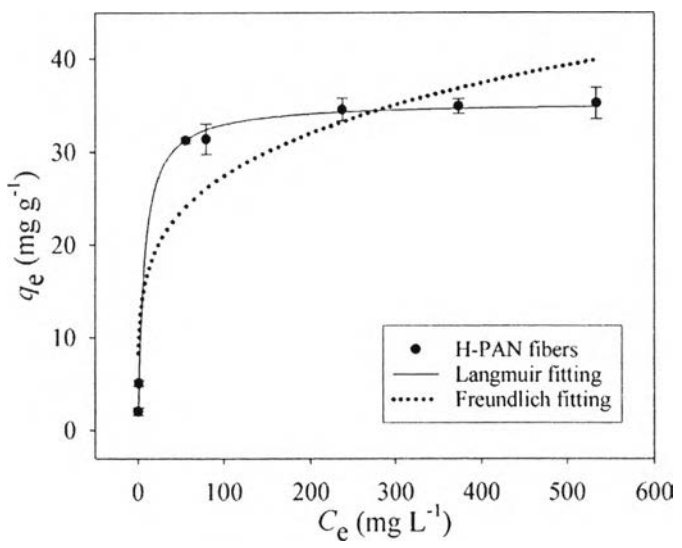

(b)

Figure 3.5 Adsorption isotherms of Cu(II) ions onto (a) H-ePAN fiber mats and (b) H-PAN fibers (n = 5). Experimental condition: initial ion concentration = 40–800 ppm, sample dose = 0.1 g/25 mL, initial pH = 5.0, temperature = 30 °C, and contact time = 24 h.

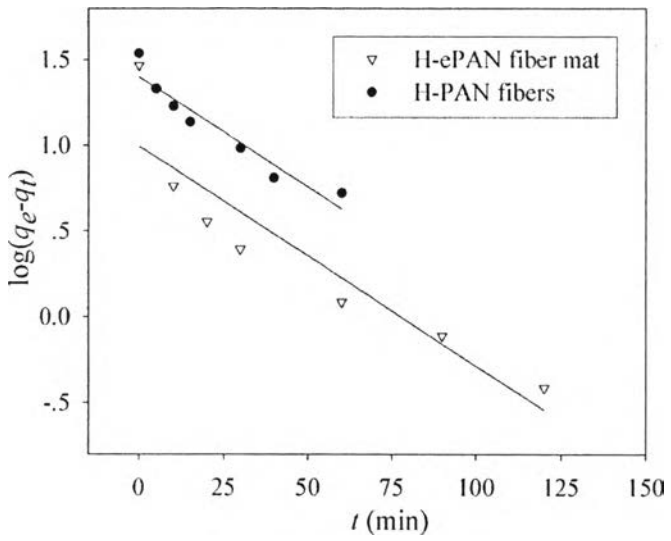

(a)

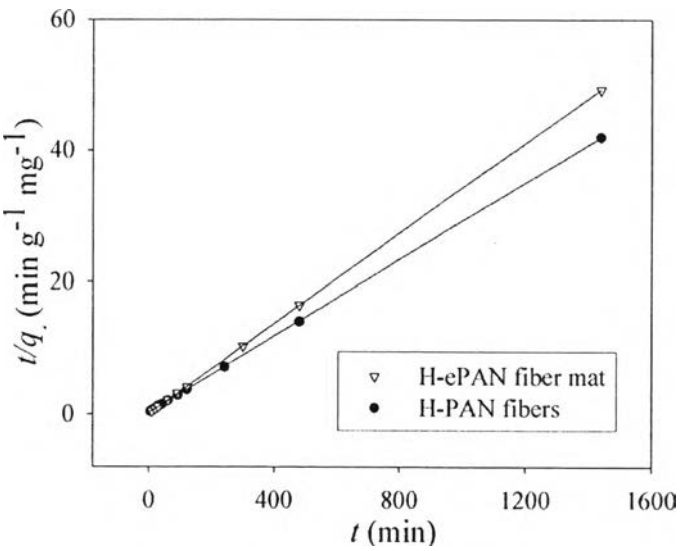

(b)

Figure 3.6 Kinetics of the adsorption of Cu(II) ions onto H-ePAN fiber mat and H-PAN fibers (see results in Figure 7), based on (a) the pseudo-first-order and (b) the pseudo-second-order kinetic models.

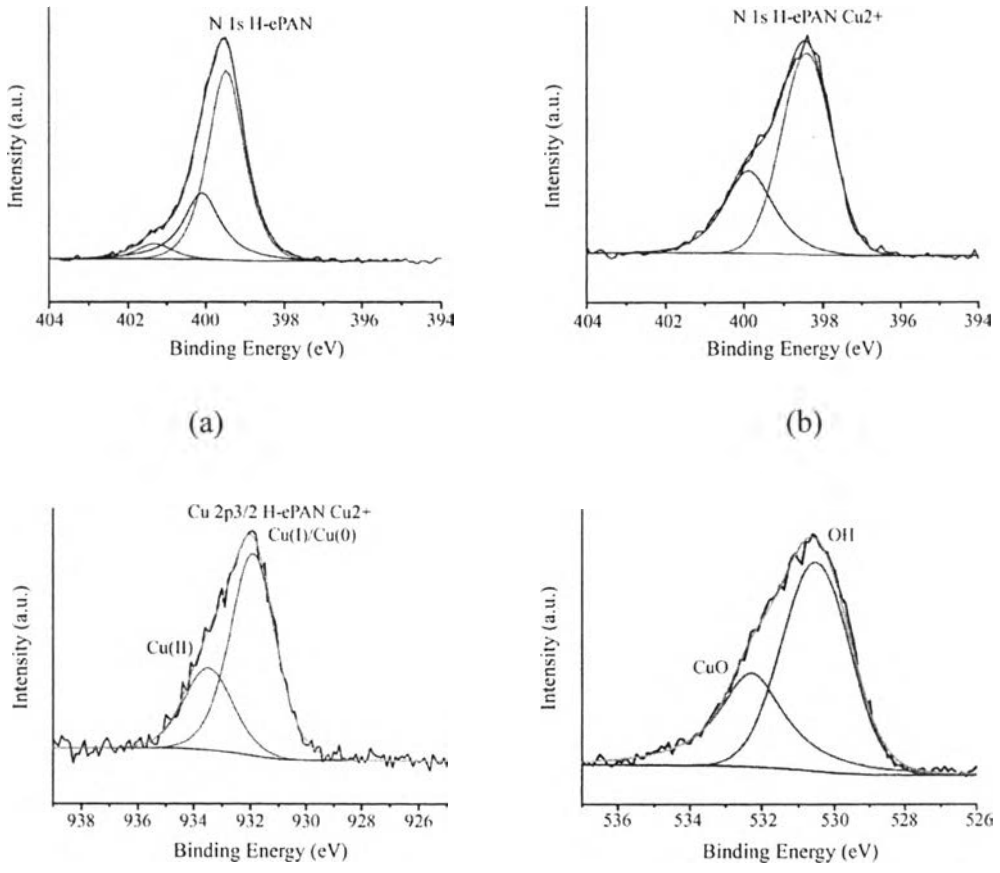

Figure 3.7 (a) N 1*s* XPS spectra of H-ePAN fiber mats before Cu(II) adsorption. (b) N 1*s* (c) Cu $2p_{3/2}$ and (d) O 1*s* XPS spectra of H-ePAN fiber mats after Cu(II) adsorption (initial ion concentration = 200 ppm, initial pH = 5.0, contact time = 24 h).